JOURNAL OF GEOPHYSICAL RESEARCH, VOL. 115, D17102, doi:10.1029/2009JD013384, 2010

Heavy rain intensity distributions on varying time scales and at different temperatures

J. O. Haerter,[1] P. Berg,[2] and S. Hagemann[1]

Received 19 October 2009; revised 22 April 2010; accepted 30 April 2010; published 3 September 2010.

[1] On the basis of observational precipitation data at a temporal resolution of 5 min from six stations in Germany we obtain scaling relations of the probability distributions of precipitation intensity with temperature and time scale. Each station record contains an approximately 30 year time series of data. By producing a cascade of averaging intervals, we obtain the behavior of precipitation intensity from the instantaneous to the daily resolution. While the intensity distribution of the shortest time scale displays a strict power law tail, it acquires a more elaborate scaling when temperatures are distinguished or when precipitation and dry periods are mixed at longer averaging intervals. The coefficient of increase with temperature is a continuously and strongly varying function of temperature and percentile and does not show an abrupt increase as noted in previous work. Conversely, when considering precipitation events, we find that the temperature dependence is reduced when the amount, not the intensity, of total precipitation produced is considered. As temperature increases, event duration decreases and reduces the accumulated precipitation yield. We caution that the Clausius-Clapeyron relation may not provide an accurate estimate of the temperature relationship of precipitation at any temporal resolution.

Citation: Haerter, J. O., P. Berg, and S. Hagemann (2010), Heavy rain intensity distributions on varying time scales and at different temperatures, *J. Geophys. Res.*, *115*, D17102, doi:10.1029/2009JD013384.

1. Introduction

[2] Precipitation events that persist throughout different time scales can lead to substantially different effects such as local flooding, erosion, and traffic disruptions on the short scales to large-scale flooding and water damage on longer scales. On the one hand, it is a difficult task to make projections of future precipitation changes due to a suspected global temperature increase [*Allan and Soden*, 2008] as a result of increased greenhouse gases. If the troposphere would warm at a rate similar to that of the surface, the vertical temperature gradient would be left relatively unchanged. Researchers have not converged on predictions of even the sign of precipitation changes as a consequence of the projected global warming [*Held and Soden*, 2006; *Solomon et al.*, 2007].

[3] On the other hand, there is additional debate about the temperature dependence of precipitation intensity in *present-day* rainfall statistics. The temperature changes we are concerned with in this paper are caused (mainly) by natural fluctuations and not by human-induced climate changes. Such temperature changes can be brought about, e.g., by the diurnal and annual cycles of solar irradiation and dynamical temperature changes. We believe that the difficulty in understanding the temperature dependence of precipitation intensity in such data lies partly in the complexity of the temporal scaling of precipitation.

[4] In general, the process of generating precipitation from atmospheric moisture is dependent on the upward motion of moist air and the rate at which the saturation value is reached in this process. One basic physical principle that has been discussed in the literature [*Allen and Ingram*, 2002; *Trenberth et al.*, 2003; *Pall et al.*, 2007; *Emori and Brown*, 2005; *Allan and Soden*, 2008] is the Clausius-Clapeyron (C-C) relation describing an increase in the atmosphere's moisture holding capacity of about 7% for a temperature rise by 1 K. Under conditions of rather constant relative humidity, precipitable water would scale with the saturation value. At least extreme precipitation, where essentially all the water already contained in the atmosphere is released, could scale with the moisture storage limit under these assumptions. However, the situation may be quite different for precipitation means where the large-scale dynamics and the atmosphere's energy budget appear to play key roles [*Allen and Ingram*, 2002]. Hence, an analysis of the entire intensity distribution function is essential.

[5] Furthermore, neither the impact of the averaging period nor the dependence on percentile becomes apparent from previous studies as they have been carried out for accumulation intervals of comparably low resolution. The temperature dependence and scaling across time scales have so far not been presented in a comprehensive way.

[6] Some recent studies have attempted to investigate changes in precipitation percentiles more quantitatively by statistical analyses of high-resolution data [*Lenderink and van Meijgaard*, 2008; *Haerter and Berg*, 2009; *Berg et al.*,

[1]Max Planck Institute for Meteorology, Hamburg, Germany.
[2]Institute for Meteorology and Climate Research, Karlsruhe Institute of Technology, Karlsruhe, Germany.

0148-0227/10/2009JD013384

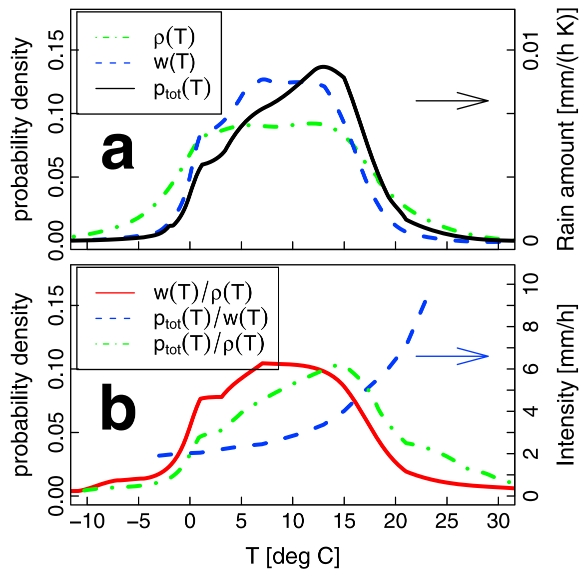

Figure 1. (a) Normalized distributions of various quantities by temperature: all occurrences $\rho(T)$, occurrences with rain $w(T)$, and total precipitation $p_{\text{tot}}(T)$ (right vertical axis). (b) Functions of the normalized distributions: probability of rain $w(T)/\rho(T)$, mean precipitation when raining $\bar{I}(T) = p_{\text{tot}}(T)/w(T)$ (right vertical axis), and mean precipitation $p_{\text{tot}}(T)/\rho(T)$. Note that $\bar{I}(T)$ is cut off at $T > 22°\text{C}$ as noise increases because of data scarcity at the highest temperatures and that units (e.g., 1/K) in probability densities are dropped for ease of presentation when clear from context.

2009]. *Lenderink and van Meijgaard* [2008] have discovered that extreme precipitation could increase at a rate twice as large as that of the C-C relation for hourly durations. The authors state several assumptions under which an increase at the C-C rate could be *expected* for the higher percentiles but find this not to be observed, especially for short time scales. *Haerter and Berg* [2009] caution that the strong increase may be due to statistical effects, and the mechanism leading to such extreme increases should be investigated further. However, both studies agree that large discrepancies may appear in data that are averaged on different time scales and that a critical inspection of the C-C comparison is required. In particular, the period over which precipitation intensity (I) is averaged, before being analyzed statistically, is of crucial importance.

[7] To address the question of changes of the entire distribution function both in relation to temperature and to the time scale, we perform a systematic statistical analysis of the scaling of temperature-conditional intensity distributions across temporal resolutions. The structure of the article is as follows. We first state the source of the data and our general statistical methods (section 2). In section 3 we discuss our results on scaling with temperature and temporal resolution. Section 4 contains a summary and states the broader implications of our work.

2. Data and Methods

[8] We have obtained time series for Germany from the stations Aachen, Göttingen, Hamburg, Kempten, Saarbrücken, and Schleswig from the German Weather Service (DWD). Throughout the text, by "precipitation interval" we mean a temporal interval that is due to the instrument resolution or averaging period. Original data were initially recorded on a chart at a resolution of $p_0 \equiv 0.1$ mm during a 5 min interval; smaller measurements are considered zero precipitation. The gauge used is of the Hellmann type, consisting of a collecting funnel of an area of 200 cm^2. The data have been quality assessed by the DWD and checked against daily sums. "Precipitation event" refers to a contiguous sequence of precipitation intervals (section 3.4).

[9] The time series from each station contains roughly 30 years of 5 min precipitation measurements and hourly temperature measurements. The total number of 5 min intervals with $p > p_0$ is 462,467. We have grouped all data into one long time series of 190 years with a precipitation and temperature measurement at time t referred to as (p_t, T_t). Hence, the time series from the different stations are taken to sample from the same statistical distribution function, and grouping them all together enhances the signal. In the present study we are not concerned with spatial correlations between the stations. For a given time scale Δt we obtain pairs of averages (I, T), with the average taken over all periods of duration Δt. We define the intensity cutoff $I_0 \equiv p_0/\Delta t$, which is the lowest measurable intensity at a given time scale Δt. To compute T-dependent quantities, we have binned all data into $\Delta T \equiv 2$ K bins and evaluated statistical quantities within each bin. To synchronize the time step to 5 min, we assume T to be constant within the hour where the measurement was taken. This approximation is sufficient as our temperature bins allow for fluctuations of up to 2 K during 1 hour. We have checked this assumption by computing the spectrum of temperature changes within 1 hour periods with and without precipitation. Binning with 4 K shows comparable results. For testing purposes, we have computed probability density functions of I for each station separately and compared the results. We find the results to vary little from station to station (not shown).

[10] Switching to a cutoff of 0.2 mm showed that the results discussed in this paper do not depend on the cutoff used. As far as the measurement precision of small measurements is concerned, we point out that the cumulative distribution of larger values will remain unchanged if their binary recording is correct. An external effect that can impact on measurement precision is strong winds. These generally impact more heavily on snow measurements, which we do not focus on in this paper.

3. Results

3.1. Mean Quantities as Function of Temperature

[11] In Figure 1 we present normalized probability density functions (PDFs) of various quantities. The distribution of all occurrences with rain (wet periods) $w(T) = \rho(T|I > I_0)$ is peaked at intermediate temperatures near 10°C. Here $\rho(T)$ is the probability distribution of all temperature measurements, irrespective of the presence of rain (Figure 1a). The mean unconditional precipitation rate (i.e., the precipitation rate averaged over wet *and* dry intervals) at a given temperature is given by $p_{\text{tot}}(T) = \int_0^\infty I'\rho_T(I')\mathrm{d}I'$, where

$$\rho_T(I) = P(I|T - \Delta T/2 < T' < T + \Delta T/2) \qquad (1)$$

specifies the normalized conditional probability of the intensity I given that the corresponding temperature T' is within the bin centered at T. The function $p_{\mathrm{tot}}(T)$ is a skewed distribution with a peak near 13°C.

[12] In Figure 1b we show ratios of these distributions. The probability of rain $w(T)/\rho(T)$, given a certain temperature, peaks and declines at lower temperatures than the mean precipitation $p_{\mathrm{tot}}(T)/\rho(T)$. Conversely, when the mean precipitation intensity during wet periods $\bar{I}(T) \equiv p_{\mathrm{tot}}(T)/w(T)$ is considered, its value increases monotonically with temperature without any sign of saturation. The ratio $w(T)/\rho(T)$ measures the likelihood of finding saturation of the atmosphere at a given temperature. At the lowest temperatures ($T < 0$°C) this likelihood is low, possibly because of the dominance of dry continental air in the region at such temperatures. At higher temperatures the contribution of moist Atlantic air is larger, and evaporation begins to add to the available moisture while the saturation vapor pressure increases. When $w(T)/\rho(T)$ begins to fall ($T > 15$°C), the available moisture possibly no longer suffices to reach the saturation level [*Berg et al.*, 2009], and mean precipitation ($p_{\mathrm{tot}}(T)/\rho(T)$) decreases. However, when it does rain, the intensity is larger ($p_{\mathrm{tot}}(T)/w(T)$). The exact explanation for the latter is part of the ongoing discussion, but hypotheses exist, e.g., in terms of avalanche-like reactions [*Peters and Neelin*, 2006].

[13] In summary, the peak in precipitation totals is due to simultaneously high $\bar{I}$ and rain probability. At lower (higher) temperatures p_{tot} falls off because of generally lower intensities (fewer rain events). Conversely, no peak is found in $\bar{I}$ as temperature increases. While the change of the probability of rain is a question by itself, we are here concerned with wet period precipitation intensity: to which extent do different percentiles of precipitation intensity depend on temperature, and how do average intensities depend on the averaging period?

3.2. Temporal Scaling of Cumulative Distributions

[14] We now direct our attention to the wet day ($I > I_0$) distribution functions of precipitation within a given temperature bin. We compute the cumulative distribution functions (CDFs)

$$\gamma_T(I) = \int_{I_0}^{I} \mathrm{d}I' \rho_T(I') \tag{2}$$

at a given time scale Δt. Here ρ_T is defined as in equation (1) but only for $I > I_0$. The CDF of total precipitation is

$$\gamma_{\mathrm{tot}}(I) = \int \mathrm{d}T w(T) \gamma_T(I), \tag{3}$$

where the integral is taken over all T. The CDFs in Figure 2a are computed from the 5 min precipitation time series. For $I > 2$ mm/h it is well approximated by a power law $\gamma_{\mathrm{tot}}(I) \propto I^{\alpha}$ + const with an exponent $\alpha \simeq -1.98$ over most of the intensity range. The proximity of α to the integer value −2 is worth mentioning. While this might be a coincidence, we note that the physical origin of the slope, such as the mechanisms of stratiform and convective precipitation, should be investigated further. The power law decay means that the likelihood of exceeding the intensity I is four times as large as that of exceeding $2I$, which indicates scale-free behavior. Hence, in the power law regime there is no "typical" intensity. This stands in marked contrast to the case of longer averaging intervals, which we discuss below. In this paper, our intent is not to engage in the ongoing detailed discussion on the scaling of $\gamma_{\mathrm{tot}}(I)$ [*Wilks*, 2006; *Vrac et al.*, 2007; *Bellone et al.*, 2000; *Katz et al.*, 2002; *Vrac and Naveau*, 2007; *Deidda et al.*, 1999; *Veneziano et al.*, 2006]. Our focus here is to analyze the behavior of conditional probabilities where temperature is restricted to a fixed range: while $\gamma_{\mathrm{tot}}(I)$ is a weighted superposition of $\gamma_T(I)$ as indicated in equation (3), the power law behavior breaks down for the functions $\gamma_T(I)$ when temperatures are distinguished. For higher values of T, the functions $\gamma_T(I)$ contribute more strongly to the high percentiles of $\gamma_{\mathrm{tot}}(I)$.

[15] To show the effect of the averaging process on the CDFs, we now rearrange our 5 min data into hourly averages. Such hourly data have been used previously [*Lenderink and van Meijgaard*, 2008]. This "coarsening" of the data already substantially changes the statistics (Figure 2b). Most strikingly, the CDF of total precipitation is no longer well approximated by a power law scaling. Furthermore, a strong shift toward weaker averaged intensities occurs at any given percentile, and the overall spread of intensities decreases between different values of T. A similar effect occurs for daily averages (Figure 2c). We note that a fit of a stretched exponential

$$1 - \gamma_{\mathrm{tot}}(I) = \exp\left[-(I/R_0)^c\right], \tag{4}$$

where R_0 is the decay constant, to the distribution of $\gamma_{\mathrm{tot}}(I)$ at the daily scale yields a coefficient $c \simeq 0.722$, a value very close to the prediction of $c = 2/3$ by *Wilson and Toumi* [2005]. Hence, at this longer time scale the scale-free character visible at the 5 min scale is lost as the exponential induces a *characteristic* intensity.

[16] The increase of I with T has recently been heavily discussed in the literature [*Allen and Ingram*, 2002; *Trenberth et al.*, 2003; *Emori and Brown*, 2005; *Pall et al.*, 2007; *Allan and Soden*, 2008; *Lenderink and van Meijgaard*, 2008; *Berg et al.*, 2009]. These studies have worked with I averaged on time scales greater than 1 hour and have only considered isolated percentiles of I. The role of the time scales involved and the dependence on percentile have therefore been hard to reconcile. We now offer an analysis where the temperature dependence and scaling across time scales are presented in a comprehensive way. To obtain the relative rate b of increase of I at a given percentile per degree Kelvin, we produce numerical derivatives

$$b(T) \equiv \frac{\partial \gamma_T}{\partial T} \frac{1}{\gamma_T} \simeq \frac{\gamma_{T+\Delta T} - \gamma_{T-\Delta T}}{2\Delta T \gamma_T} \tag{5}$$

for all percentiles. Figure 2d shows b for all T and percentiles for the 5 min data. As percentiles approach zero, b also goes to zero, and it reaches its highest values of $\simeq$0.2 for the highest percentiles. Generally, b increases with T, except for the very highest T and percentiles, where it again decreases. In Figure 2d we also indicate the increase of 0.07

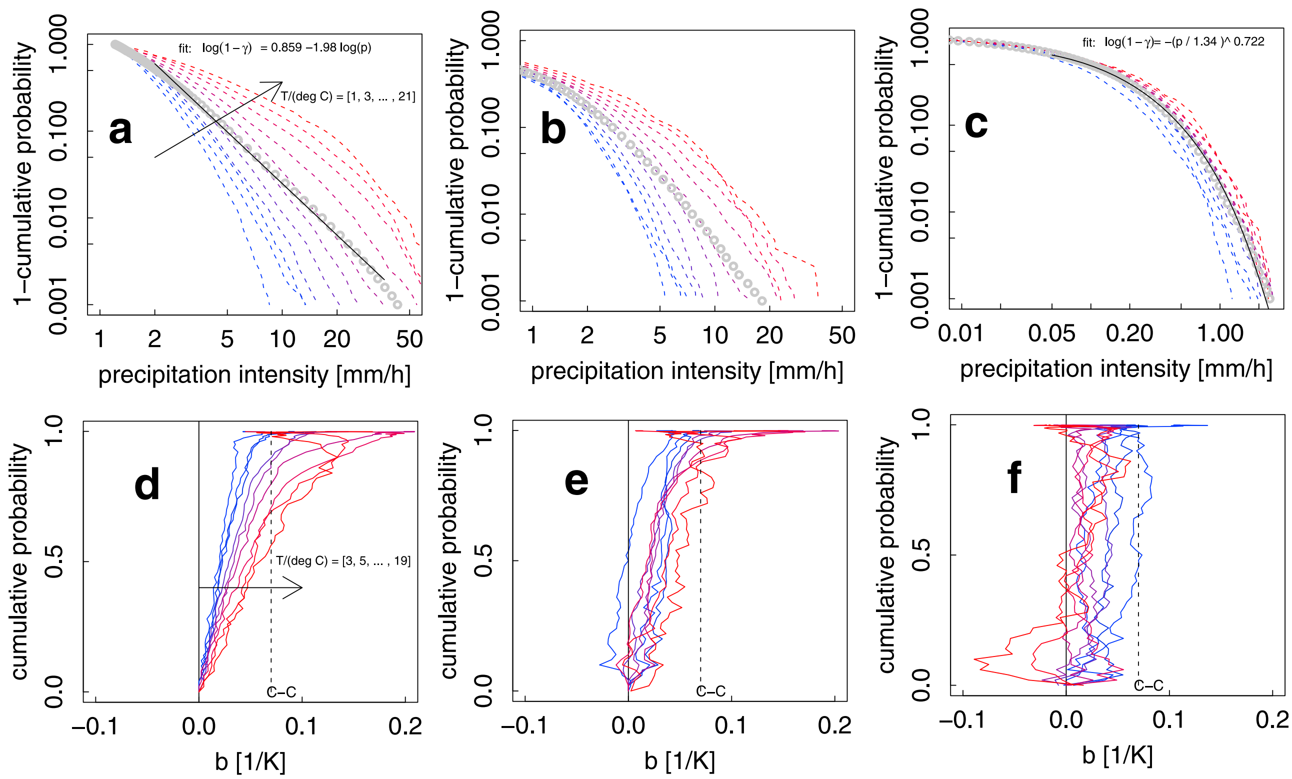

Figure 2. (a) Cumulative distribution function of I conditional on T (colors from blue to red correspond to increasing $T = [1, \ldots, 21]$°C) and of total precipitation (gray circles). The latter is fitted by a power law (solid line), with double log scale chosen to enhance presentation of higher percentiles. (b) Same as Figure 2a but for hourly averaging of I. (c) Same as Figure 2a but for daily averaging. Fit is a stretched exponential. (d–f) Corresponding relative change b of distribution function with T. Curves are partial numerical derivatives with respect to temperature for $T = [3, \ldots, 19]$°C, and the dotted vertical black lines show a Clausius-Clapeyron increase of 0.07/K. Curves in Figures 2e and 2f become more erratic because of the reduction of data; at $\gamma = 0$ the cutoff I_0 confines curves to zero.

that would result for all T if the C-C relation could be used as an indicator of precipitation increases. On the hourly scale (Figure 2e) substantial differences were yielded: the overall increase with T is much weaker, and the curves of different T are not as clearly separated. While *Lenderink and van Meijgaard* [2008] have argued for abrupt increases of b to twice the C-C value at this averaging interval at the highest percentiles, we note that the increase of b is rather continuously increasing with T and percentile, except for the very highest temperatures. On a daily time scale (Figure 2f) the T dependence of b is now actually reversed with lower T displaying larger coefficients. Furthermore, most percentiles show similar values of b between 0 and 0.07.

3.3. Scaling of Percentiles With Temporal Resolution

[17] To better understand Figures 2d–2f, we further investigate the scaling of percentiles with temporal resolution Δt for different T (Figure 3). Precipitation intensity strongly depends on Δt. This is due to two effects: the appearance of dry intervals during the longer averaging times which substantially reduce the mean intensities and the mixing of wet intervals of different intensities within a single event. As a result, the scaling from 5 min to 1 day cannot be described by a unique scaling function. A change of scaling occurs near 30 min: at intervals less than 30 min we find a good fit with exponential scaling (Figure 3a), while at longer periods the scaling is well described by a power law (Figure 3b).

[18] In a separate analysis we have investigated PDFs of precipitation event duration using intermittency times (interrupting dry intervals) ranging from 0 to 180 min; hence, we have allowed for short interruptions of the contiguous precipitation sequence. Typically, event durations are 30–60 min, and events at higher T are generally shorter (Figure 4b and section 3.4). The behavior at $\Delta t < 30$ min is predominantly due to mixing of precipitation intensities within a single event (Figure 3). Conceptually, one can understand this behavior by randomly drawing data from the colored curves in Figure 2a and averaging them. Collecting the averages leads to the construction of a new distribution similar to that in Figure 2b. Such averaging leads to a decreased range of the resulting intensity values and a convergence toward mean intensity for very long event durations. However, as the longer averaging interval may also contain dry intervals, an additional general shift toward lower intensities occurs.

[19] At Δt longer than 30–60 min, the predominant effect is the inclusion of more and more nonprecipitating intervals. Hence, the scaling is roughly the trivial $I(\Delta t) = p_{\text{event}}/\Delta t$,

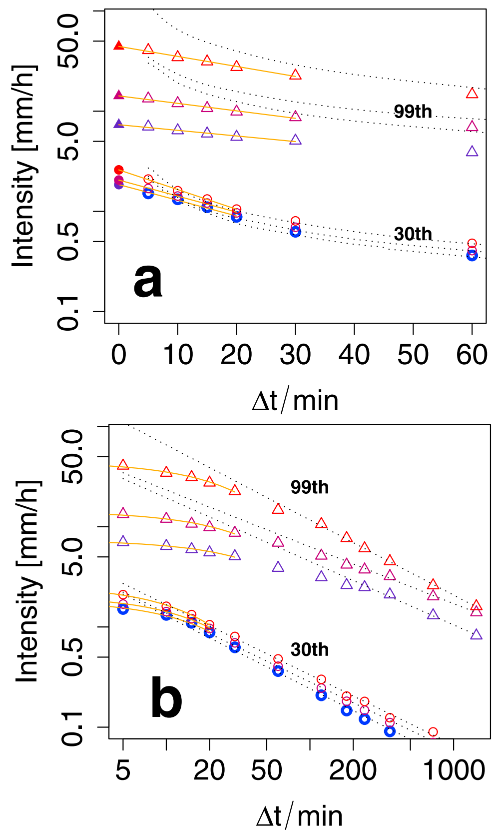

Figure 3. Scaling of percentiles with Δt. Symbols correspond to 99th (triangles) and 30th (circles) percentiles, and colors from blue to red correspond to $T = \{3, 11, 19\}$°C. (a) A log linear plot for the time period 0–60 min. (b) A log-log plot for time periods from 5 min to 1 day. Orange lines are exponential fits to the data points up to 30 min. Solid symbols at $\Delta T = 0$ in Figure 3a correspond to extrapolated instantaneous intensities. Dotted black lines are power law fits to data beyond 30 min.

where p_{event} is the accumulated event precipitation. Note that small deviations from the clean $1/\Delta t$ occur, possibly because of the occurrence of additional precipitation events (separated by dry periods) or less frequent extended events. The transition between an exponential behavior and the power law behavior occurs at smaller Δt for higher T. This is due to the shorter duration of events at higher T (Figure 4b).

[20] By extrapolating the exponential fit

$$I(\Delta t, T, \gamma) \equiv I^{\text{inst}}(T, \gamma)\ \exp\left[-c(T, \gamma)\Delta t\right]$$

to instantaneous time periods ($\Delta t \to 0$), we are able to construct the probability distribution of instantaneous precipitation intensity $I^{\text{inst}}(T, \gamma)$ (not shown). The result is similar to Figure 2a with only a small overall shift toward higher intensities. When the curve of $\gamma_{\text{tot}}(I^{\text{inst}})$ is considered in this case, the power law fit is even slightly better than in the 5 min case. This result may aid in construction of high-resolution weather generators. By extracting the coefficient $c(T, \gamma)$ from the fit, we obtain the decay coefficient as a function of T and percentile (Figure 4a). Here $c(T, \gamma)$ describes the rate of decrease of the intensity at a given percentile with an increasing averaging interval Δt. There is a generally faster decay for higher temperatures. This is due to the shape of the distribution functions where the extremes increase more strongly with T than the means. Hence, by approaching the means through the averaging procedure, the magnitude of the decay coefficient must be larger for higher T. When lower percentiles are considered, the coefficient decreases.

[21] In a similar way we can understand the transition between the time scales shown in Figures 2d–2f. As the averaging period is increased from Δt to $\Delta t'$, several precipitation intervals are drawn from the distribution corresponding to Δt and a given T (colored curves) and are averaged. Such averaging weakens (strengthens) increases at the higher (lower) percentiles. When proceeding beyond the typical event duration of the chosen temperature, generally dry periods are mixed in with the average. As high temperatures come with shorter event durations, a reversal of the order of the temperature curves occurs in Figure 2f. A

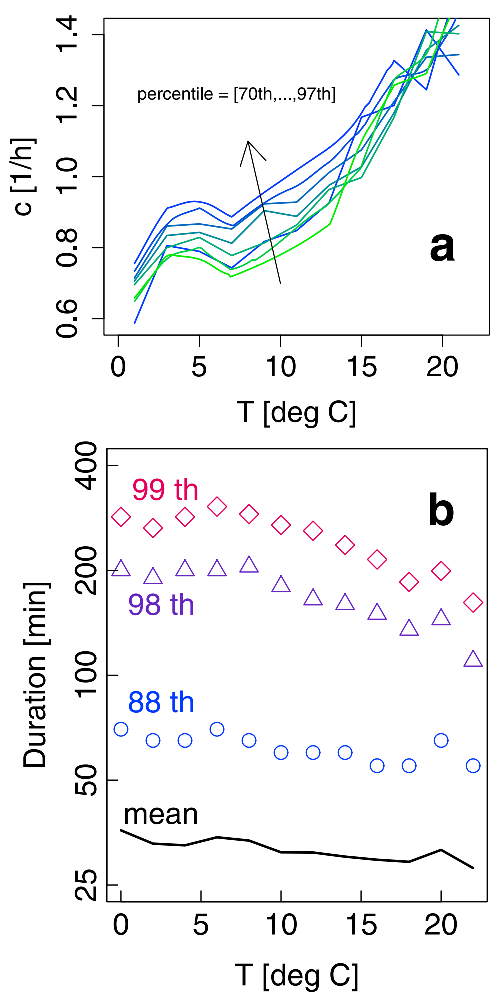

Figure 4. (a) Decay coefficients extracted from fits in Figure 3a as a function of temperature T. Colors from green to blue correspond to 70th to 97th percentiles. (b) Percentiles and mean of event duration versus event onset temperature T. Note the logarithmic vertical axis.

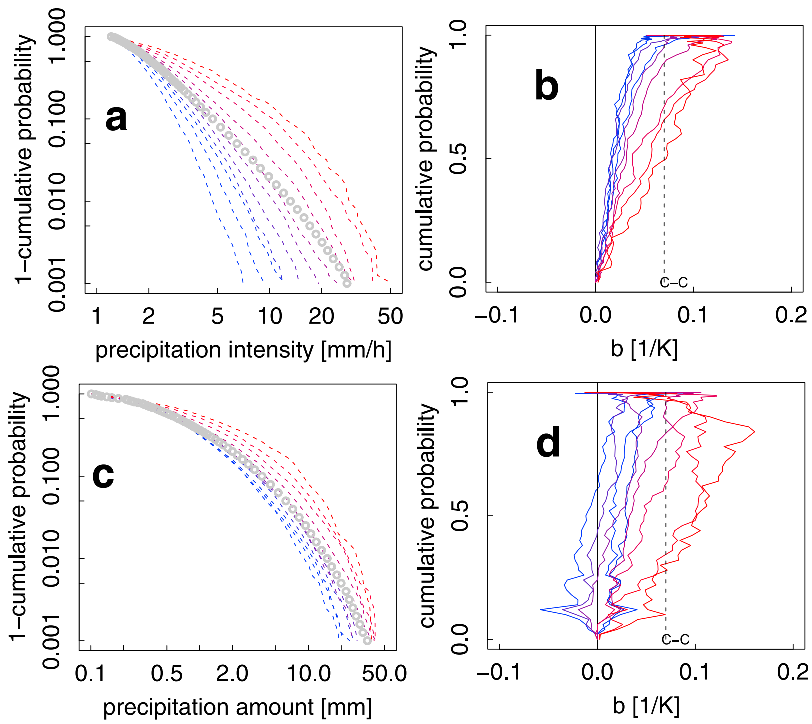

Figure 5. (a, b) Same as Figure 2 but for mean event precipitation intensity and event onset temperature. (c, d) Same as Figures 5a and 5b but for total event precipitation amount.

further effect that may contribute to this is an event-induced cooling off for long event durations.

3.4. Event-Based Analysis

[22] In this section we investigate precipitation events, as opposed to fixed intervals in sections 3.2 and 3.3. An event is taken as a contiguous sequence of precipitation intervals; however, a number of interrupting intervals (intermittency) with $p < p_0$ are allowed [*Dunkerley*, 2008]. We use intermittency times between 0 and 180 min. The results are similar, and we show only plots for an allowed intermittency of 60 min. Such intermittencies are not counted toward event duration. We reproduce Figures 2a and 2b for the mean event intensities (Figures 5a and 5b). Clearly, the absolute magnitude of intensities decreases considerably when comparing to Figure 2a. This is due to the averaging of intensities within the event as described in section 3.3 and Figure 3a. When comparing the spread of intensities for the highest and lowest temperatures, we find only a small decrease of their ratio compared to the 5 min data (ratio $\simeq 7$). This is also reflected in the temperature derivatives in Figure 5b.

[23] A rather different picture results when we consider the statistics of the total *precipitation amount* produced throughout the events (Figure 5c). The relative spread of precipitation amount is now generally much smaller (ratio $\simeq 2.5$). While there is an increase of event precipitation amount with temperature (Figure 5d), this increase is weaker than for the mean event intensities, especially for the lower temperatures. This weakening of the increase with temperature is due to the temperature dependence of event duration (Figure 4b). While event duration is rather constant below 6°C, it falls off to about two thirds of its value near 22°C. The drop may be caused by a combination of several effects: shorter cloud lifetime at higher temperatures, smaller cloud size (especially for convective events), and rapid cloud advection away from the observer. The first of these explanations is in line with an argument based on atmospheric moisture availability presented by *Berg et al.* [2009]. In that study an analysis of model data showed that on precipitating days the moisture amount in the atmospheric column does not increase as rapidly as the atmosphere's ability to store moisture. The resulting discrepancy may then lead to shorter event durations and even decreases in daily precipitation amount with temperature, e.g., in the midlatitude summer.

4. Discussion and Conclusion

[24] Using long time series of 5 min precipitation data, we have studied the complex temperature relation of precipitation intensity distributions as the time scale is varied. Temporally averaged at the daily time scale, increases in precipitation intensity generally below the Clausius-Clapeyron rate are found with systematically lower increases at higher temperatures. Conversely, at the 5 min temporal resolution the increases are much more pronounced and depend strongly on temperature. We note, however, that at the daily scale the Clausius-Clapeyron relation may constitute an upper bound for the increase.

[25] Our results show that precipitation intensity has a systematic dependence on temperature. However, the undertaking of drawing simple conclusions for precipitation intensity changes with temperature from the Clausius-Clapeyron relation alone can be discouraged as a conclusion of our analysis. While moisture increases in the atmosphere may be

closely related to temperature increases (assuming constant relative humidity), we emphasize that such simple relations do not apply for precipitation. We encourage a thorough investigation of the origin of the distribution functions of precipitation intensity $\gamma_T(I)$ and their relation to the cloud water and rain formation process at a given relative humidity. Such analysis may be aided by combining data from remote sensing missions with those of ground-based observations.

[26] Besides thermodynamic effects, dynamical effects may have important consequences on the distribution functions of precipitation intensity. When precipitation events are considered, a systematic decrease of event duration with temperature leads to less dramatic increases of the amount of precipitation yielded by a single event as compared to the increases found in the case of the mean event intensity. This aspect has to be taken into account when deriving risk assessments from precipitation-temperature statistics.

[27] Concerning the diurnal cycle, we have found in a separate analysis that distribution functions constrained to temperature show increases in extremes during the late afternoon. We attribute such behavior to the buildup of moisture and subsequent microphysical processes in clouds throughout the day. Hence, changes in the diurnal cycle or other processes that allow the buildup of moisture or convective energy in a warming climate may be equally as important as the temperature change alone as far as precipitation intensity is concerned.

[28] **Acknowledgments.** We acknowledge partial financial support by the EU project WATCH (contract 036946). P. Berg acknowledges financing from the CEDIM project. We thank J. Quaas for fruitful discussions. The authors acknowledge Deutscher Wetter Dienst (DWD) for provision of observational data.

References

Allan, R. P., and B. J. Soden (2008), Atmospheric warming and the amplification of precipitation extremes, *Science*, *321*, 1481–1484.

Allen, M. R., and W. J. Ingram (2002), Constraints on future changes in climate and the hydrologic cycle, *Nature*, *419*, 224–232.

Bellone, E., J. P. Hughes, and J. P. Guttorp (2000), A hidden Markov model for downscaling synoptic atmospheric patterns to precipitation amounts, *Clim. Res.*, *15*, 1–12.

Berg, P., J. O. Haerter, P. Thejll, C. Piani, S. Hagemann, and J. H. Christensen (2009), Seasonal characteristics of the relationship between daily precipitation intensity and surface temperature, *J. Geophys. Res.*, *114*, D18102, doi:10.1029/2009JD012008.

Deidda, R., R. Benzi, and F. Siccardi (1999), Multifractal modeling of anomalous scaling laws in rainfall, *Water Resour. Res.*, *35*, 1853–1867.

Dunkerley, D. (2008), Identifying individual rain events from pluviograph records: A review with analysis of data from an Australian dryland site, *Hydrol. Processes*, *22*, 5024–5036.

Emori, S., and S. J. Brown (2005), Dynamic and thermodynamic changes in mean and extreme precipitation under changed climate, *Geophys. Res. Lett.*, *32*, L17706, doi:10.1029/2005GL023272.

Haerter, J. O., and P. Berg (2009), Unexpected rise in extreme precipitation caused by a shift in rain type?, *Nat. Geosci.*, *2*, 372–373.

Held, I., and B. J. Soden (2006), Robust responses of the hydrological cycle to global warming, *J. Clim.*, *19*, 5686–5699.

Katz, R., M. B. Parlange, and P. Naveau (2002), Statistics of extremes in hydrology, *Adv. Water Resour.*, *25*, 1287–1304.

Lenderink, G., and E. van Meijgaard (2008), Increase in hourly precipitation extremes beyond expectations from temperature changes, *Nat. Geosci.*, *1*, 511–514.

Pall, P., M. R. Allen, and D. A. Stone (2007), Testing the Clausius-Clapeyron constraint on changes in extreme precipitation under CO_2 warming, *Clim. Dyn.*, *28*, 351–363.

Peters, O., and J. D. Neelin (2006), Critical phenomena in atmospheric precipitation, *Nat. Phys.*, *2*, 293–296.

Solomon, S., et al. (Eds.) (2007), *Climate Change 2007: The Physical Science Basis: Contribution of Working Group I to the Fourth Assessment Report of the Intergovernmental Panel on Climate Change*, 996 pp., Cambridge Univ. Press, Cambridge, U. K.

Trenberth, K. E., A. Dai, R. M. Rasmussen, and D. B. Parsons (2003), The changing character of precipitation, *Bull. Am. Meteorol. Soc.*, *84*, 1205–1217.

Veneziano, D., A. Langousis, and P. Furcolo (2006), Multifractality and rainfall extremes: A review, *Water Resour. Res.*, *42*, W06D15, doi:10.1029/2005WR004716.

Vrac, M., and P. Naveau (2007), Stochastic downscaling of precipitation: From dry events to heavy rainfalls, *Water Resour. Res.*, *43*, W07402, doi:10.1029/2006WR005308.

Vrac, M., M. Stein, and K. Haydoe (2007), Statistical downscaling of precipitation through a nonhomogeneous stochastic weather typing approach, *Clim. Res.*, *34*, 169–184.

Wilks, D. S. (2006), *Statistical Methods in the Atmospheric Sciences*, 2nd ed., Elsevier, Oxford, U. K.

Wilson, P. S., and R. Toumi (2005), A fundamental probability distribution for heavy rainfall, *Geophys. Res. Lett.*, *32*, L14812, doi:10.1029/2005GL022465.

P. Berg, Institute for Meteorology and Climate Research, Karlsruhe Institute of Technology, D-76021 Karlsruhe, Germany.

J. O. Haerter and S. Hagemann, Max Planck Institute for Meteorology, Bundesstr. 53, D-20146 Hamburg, Germany. (jan.haerter@zmaw.de)